Dalton Transactions

Check for updates

Access to 1,2,3-triphospholide ligands by reduction of di-*tert*-butyldiphosphatetrahedrane†

Maria K. Uttendorfer, [ID] Gabriele Hierlmeier, [ID] ‡ Gábor Balázs [ID] and Robert Wolf [ID] *

Di-*tert*-butyldiphosphatetrahedrane (tBuCP)$_2$ (**A**) is a reactive tetrahedral molecule which may serve as a source of new phosphaorganic molecules and ligands. However, the redox chemistry of this compound has not yet been investigated. Here, we show that the reduction of **A** with alkali metals (AM = Li, Na, K, Rb and Cs) affords 1,2,3-triphospholides [AM(crown ether)][1,2,3-P$_3$C$_2t$Bu$_2$] (**1–5**, [AM(crown ether)] = [Li([12] crown-4)$_2$]$^+$, [Na([15]crown-5)$_2$]$^+$, [K([18]crown-6)]$^+$, [Rb([18]crown-6)]$^+$, and Cs$^+$) with 1,3-diphospholides [AM(crown ether)][1,3-P$_2$C$_3t$Bu$_3$] (**6–10**) formed as by-products. The potassium salt **3** was isolated on a preparative scale, allowing for reactivity studies. Transmetalation with iron(II) and ruthenium(II) chlorides yielded the sandwich complexes [Cp*M(η^5-1,2,3-P$_3$C$_2t$Bu$_2$)] (**11**, M = Fe; **12**, M = Ru, Cp* = C$_5$Me$_5$) featuring η^5-coordinated triphospholide ligands. Treatment of **3** with [Cp$_2$Fe][BAr$_4$^{F}] or [H(Et$_2$O)$_2$BAr$_4$^{F}] (BAr$_4$^{F} = B{C$_6$H$_3$(CF$_3$)$_2$}$_4$) afforded the polyphosphorus compound tBu$_4$C$_4$P$_6$ (**13**), which presumably results from the dimerisation of a 1,2,3-triphospholyl radical intermediate (1,2,3-P$_3$C$_2t$Bu$_2$)$^·$ (**3$^·$**). Tetracyclic **13** is closely structurally related to an isomer of the hydrocarbon hypostrophene (C$_{10}$H$_{10}$).

Introduction

Phosphatetrahedranes can be used to illustrate the diagonal relationship between carbon and phosphorus in the periodic table, and were postulated as stable compounds decades ago.[1,2] Surprisingly, the first representatives for this class of tetrahedral molecules were reported only recently.[3–5] We described the synthesis of di-*tert*-butyldiphosphatetrahedrane (tBuCP)$_2$ (**A**, Fig. 1a) *via* the nickel-catalysed dimerisation of the phosphaalkyne tBuCP.[3] In parallel, Cummins and co-workers synthesised and explored the reactivity of tri-*tert*-butyl-phosphatetrahedrane (tBu$_3$C$_3$P) (**B**) and triphosphatetrahedrane (HCP$_3$) (**C**).[4,5] The phosphatetrahedranes **A–C** are isolobal to purely carbon-based tetrahedranes such as (tBuC)$_4$ (**D**), and the classical "inorganic tetrahedrane" P$_4$ (**E**, white phosphorus).[6,7] This has inspired the study of the reaction chemistry of **A–C**, which has revealed some similarities, but also differences with respect to the chemistry of white phosphorus in particular.[3–5,8–14]

Isomerisations of the phosphatetrahedrane scaffold have been observed in reactions with main group nucleophiles. Thus, N-heterocyclic carbenes (NHCs) effect P–C or P–P bond cleavage in **A**, giving bis(phosphaalkenes) or phosphirenes depending on the NHC (Fig. 1b).[8] An isomerisation of **B** to intermediary (tri-*tert*-butylcyclopropenyl)phosphinidene has been proposed for various reactions, *e.g.* with triphenylmethyl-enephosphorane and a base-stabilized silylene.[9] The isomerisation to transient phosphacyclobutadienes is another predominant reaction path, which has been reported for the irradiation of **A** by UV or visible light and for the reaction of **B** with Lewis acids (Fig. 1b).[10,11] Cyclobutadiene-type ligands are formed directly on the metal atom when **A** interacts with various low-valent Fe, Co and Ni complexes (Fig. 1b).[12,13] Further studies have shown that phosphatetrahedranes may alternatively retain their tetrahedral structure in selected coordination compounds.[3,5,14]

To the best of our knowledge, there are no reports on the synthesis of organophosphorus anions by reduction of phosphatetrahedranes. In contrast, the reduction chemistry of the closely-related compounds P$_4$ (**E**) and *tert*-butyl-phosphaalkyne (tBuCP, the monomer of **A**) is well-investigated.[15–19] Reactions of P$_4$ with sodium afford penta-phospholide, tetraphospholide and 1,2,3-triphospholide anions (among other polyphosphide species),[15,16] while reduction of phosphaalkynes (RCP) with Na/Hg (and other alkali metal reductands) yields di- and 1,2,4-

Institute of Inorganic Chemistry, University of Regensburg, 93053 Regensburg, Germany. E-mail: robert.wolf@ur.de

Results and Discussion

Reduction of A with alkali metals: synthesis and characterisation of triphospholides 1–5

Initially, the redox properties of $(t\text{BuCP})_2$ (**A**) were investigated by cyclic voltammetry in toluene/THF/[$n\text{Bu}_4\text{N}$]PF$_6$. Surprisingly, no redox process was observed between −3.0 and +1.2 V *vs.* Fc/Fc$^+$ (Fc = Cp$_2$Fe, see Fig. S47, ESI†). The absence of any redox wave suggests that strong oxidants and reductants are required to react with **A**, while also indicating that oxidation and reduction is likely associated with a large overpotential on the platinum working electrode. DFT calculations on **A** show that the HOMO lies higher and the LUMO lower in energy compared to P$_4$.[11] This suggests that, in principle, **A** should be more easily reduced and oxidized. P$_4$ can be reduced at the potential $E_{1/2}$ = −1.55 V (*vs.* bottom mercury in DMF).[30] Therefore, the chemical reduction of **A** was pursued.

Different reducing agents were evaluated in experiments performed on an NMR scale. Unfortunately, **A** did not react with magnesium or zinc powder. Activated Rieke zinc and Rieke magnesium gave black and brown suspensions, respectively. The reaction with Rieke zinc is very unselective, leading to an array of unidentified products according to ^{31}P NMR spectroscopy. In contrast, the ladderane $(t\text{BuCP})_4$ was observed as main product in the reaction with Rieke magnesium. $(t\text{BuCP})_4$ is the dimerisation product of **A**, which can also be obtained by irradiation with UV or visible light (Fig. 1b).[11,31]

The use of strongly reducing alkali metals gave more promising results. Analysis of the ^{31}P{^{1}H} NMR spectrum of the reaction of **A** with lithium chunks showed full consumption of **A** and two new species in a 2 : 1 ratio (see Fig. S1, ESI†). After the addition of [12]crown-4, these species were identified as [Li([12]crown-4)$_2$][1,2,3-P$_3$C$_2t$Bu$_2$] (**1**) and [Li([12]crown-4)$_2$][1,3-P$_2$C$_3t$Bu$_3$] (**6**, Scheme 1) based on the comparison of the NMR spectroscopic data with related compounds.[18,20–29] The major product **1** is characterized by two doublets of doublets at 224.0 ppm and 316.2 ppm ($^1J_{AX}$ = −463.8 Hz, $^1J_{A'X}$ = −465.5 Hz, $^2J_{AA'}$ = 4.3 Hz), while **6** gives rise to a singlet at 196.0 ppm (see Fig. S6, ESI†). Subsequent investigations using heavier
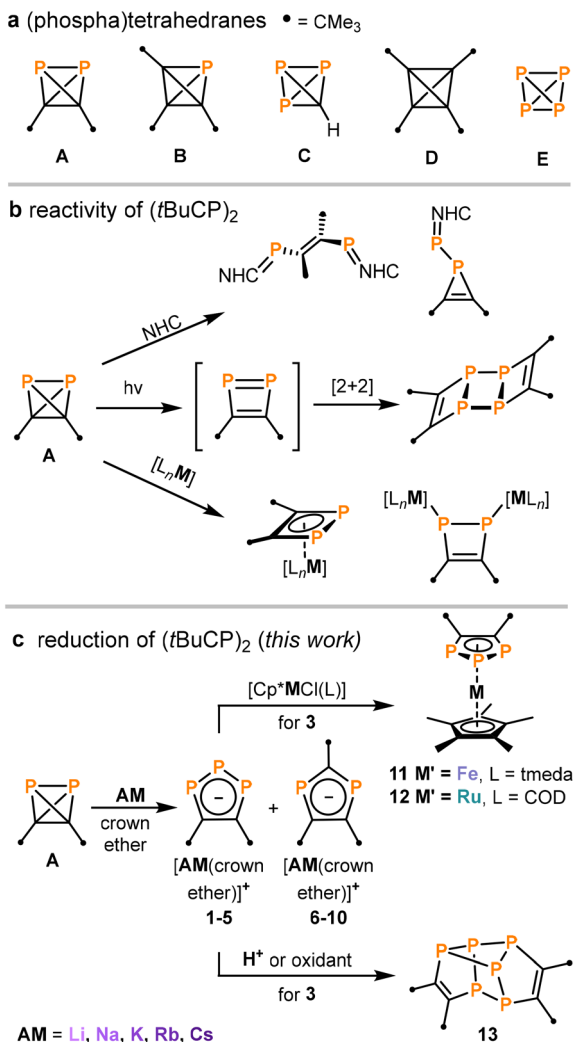

Fig. 1 (a) Tetrahedranes comprised of phosphorus and carbon atoms;[3–7] (b) reactivity of **A** (NHC = N-heterocyclic carbene, M = Fe, Co, Ni; L *e.g.* 1,5-cyclooctadiene, anthracene, cyclopentadienyl),[8,11–13] (c) alkali metal reduction of **A** and subsequent reactivity studies.

triphospholides.[17–19] These previous results inspired us to explore similar reductions of $(t\text{BuCP})_2$ (**A**) (Fig. 1c), with the aim to access anionic ligands. Here, we report the synthesis of 1,2,3-triphospholide salts [AM(crown ether)][1,2,3-P$_3$C$_2t$Bu$_2$] (**1–5**, [AM(crown ether)] = [Li([12]crown-4)$_2$]$^+$, [Na([15]crown-5)$_2$]$^+$, [K([18]crown-6)]$^+$, [Rb([18]crown-6)]$^+$, and Cs$^+$) from **A** and alkali metals. The utility of **3** as a suitable precursor for 1,2,3-triphospholide complexes is demonstrated by coordination to group 8 metal complexes. Furthermore, we report the synthesis and characterisation of the unusual polyphosphane $(t\text{Bu}_4\text{C}_4\text{P}_6)$ (**13**), which is an oxidation product of **3** with a remarkable structure built up by two fused 1,2,3-triphospholyl units. Our results complement previous studies on the synthesis of 1,2,3-triphospholides *via* several other routes, including most prominently the reaction of polyphosphide anions with alkynes.[16,20–29]
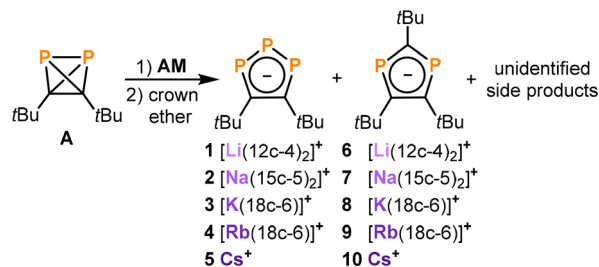

Scheme 1 Reduction of di-*tert*-butyldiphosphatetrahedrane (**A**) yielding the triphospholides **1–5** as the major products next to the diphospholides **6–10** and other unidentified side products (AM = Li, Na, K, Rb, Cs, 12c-4 = [12]crown-4, 15c-5 = [15]crown-5, 18c-6 = [18]crown-6). Conditions: THF, −80 °C → r.t., over night.

alkali metals (Na–Cs) gave similar mixtures of the tri- and diphospholide (Scheme 1).

Salts **1–10** clearly result from the initial reduction of **A**, followed by rearrangements that involve the exchange of P and C*t*Bu units.§ A similar process has been reported in the literature for the related reduction of *t*BuCP, but this yields mixtures of 1,2,4-triphospholides and 1,3-diphospholides.[18] 1,2,4-Triphospholides have been studied far more intensely than their 1,2,3-isomers due to the easier synthetic accessibility. The first 1,2,3-triphospholide salt was reported by Baudler and co-workers in 1990 as a side product in the reaction of P_4 with sodium in diglyme.[16] Since then several other 1,2,3-triphospholides have been reported, which contain aryl, alkyl, ester groups or hydrogen atoms as substituents.[20–29]

It is interesting to note that the ratio of di- and triphospholide in this reaction mixture does not reflect the ratio of carbon and phosphorus atoms in the starting material **A**. Thus, several unidentified side products were detected in the ^{1}H NMR spectra of the reaction mixtures, among them a singlet at 1.15 ppm which likely can be attributed to the remaining *t*BuC fragments of this reaction (see Fig. S11, ESI†). The similar solubility of the di- and triphospholide salts hampers their clean isolation. Gratifyingly, salts **1** and **3** were isolated as crystalline materials in varying yield of up to 5% and 32%, respectively, whereas attempts to cleanly isolate **2**, **4** and **5** gave mixtures featuring the di- and triphospholide (see the ESI† for further details).

The molecular structures of the di- and triphospholide salts are corroborated by single-crystal X-ray diffraction (sc-XRD) studies on crystals of **1**, **3**, **4** and **9** obtained from *n*-hexane/THF or *n*-hexane/toluene. The molecular structure of potassium salt **3** is shown as an example in Fig. 2a. The similar structures of the lithium and rubidium triphospholides **1** and **4** and the structure of the rubidium diphospholide **9** are shown in the ESI.† The salient feature of the structures of **1**, **3** and **4** are the planar five-membered P_3C_2 rings which are consistent with an aromatic 6 π-electron ring system with bond lengths in between typical single and double bonds (*e.g.* **3**: C–C (1.420(3) Å), C–P (1.780(2) Å), P–P (2.0740(8) Å and 2.0777(8) Å)). This is well in line with related triphospholide structures.[16,20,23,25,26,29,32]

In contrast to other symmetrically substituted triphospholide salts,[16,20,25,27,29] the ^{31}P{^{1}H} NMR spectra of **1–5** do not display an A_2B spin system but an AA′X spin system. For example, the simulation of the spin system for **3** by an iterative fitting procedure gave the PP coupling constants: $^1J_{AX}$ = 465.6 Hz, $^1J_{A'X}$ = 467.5 Hz and $^2J_{AA'}$ = 4.3 Hz (Fig. 2b). The magnetic inequivalence of the phosphorus atoms P^A and $P^{A'}$ is likely due to the proximity of the *t*Bu groups which cannot rotate independently and thus differentiates the two otherwise symmetrical halves of the 1,2,3-triphospholide anion (see Fig. S44, ESI†). The ^{31}P{^{1}H} NMR spectrum of **3** did not change significantly at elevated temperature (25, 40 and
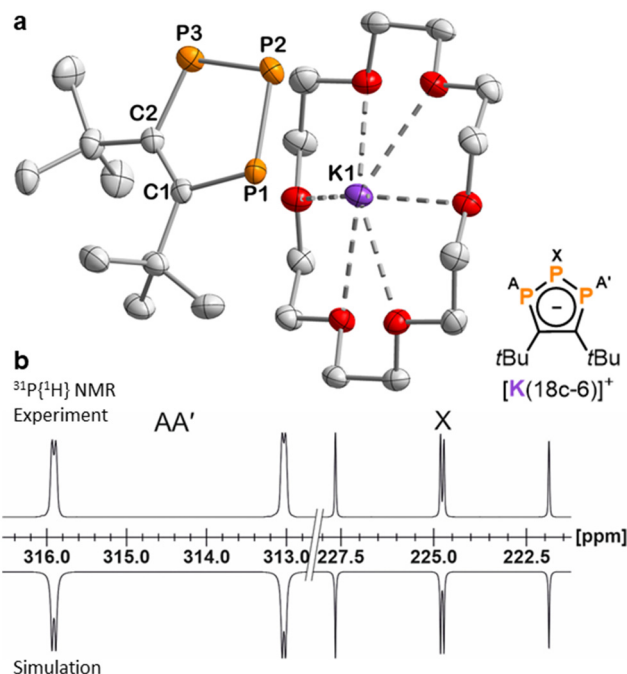

Fig. 2 (a) Solid-state molecular structure of **3**. Displacement ellipsoids are drawn at the 50% probability level; H atoms have been omitted for clarity. Selected bond lengths [Å] and angles [°]: P1–P2 2.0777(8), P2–P3 2.0740(8), P1–C1 1.780(2), P3–C2 1.780(2), C1–C2 1.420(3), P1–P2–P3 97.24(3), C1–P1–P2 102.86(8), C2–P3–P2 103.02(7), C2–C1–P1 118.52(16), C1–C2–P3 118.35(15). (b) Section of the ^{31}P{^{1}H} NMR spectrum of **3** with nuclei assigned to an AA′X spin system; experimental (top); simulation (bottom): $\delta(P_X)$ = 224.8 ppm, $\delta(P_{AA'})$ = 314.4 ppm, $^1J_{AX}$ = −465.6 Hz, $^1J_{A'X}$ = −467.5 Hz, $^2J_{AA'}$ = 4.3 Hz. The ^{31}P{^{1}H} NMR spectrum of **1** is similar (see the ESI† for further details).

60 °C), which may indicate that the *t*Bu-groups rotate in a concerted fashion (see Fig. S19, ESI†). The ^{1}H NMR spectrum of **3** gives two partly overlapping singlets for the *t*Bu groups at 1.75 ppm, similarly attributed to the non-equivalence of the 18 hydrogen atoms due to the hindered rotation of the *t*Bu groups. Another singlet at 3.57 ppm arises from the hydrogen atoms of the crown ether molecule. The signal of the carbon nuclei in the five-membered P_3C_2 core of **3** appears as a multiplet centred at 184.4 ppm in the ^{13}C{^{1}H} NMR spectrum, due to coupling to the phosphorus atoms. The multiplet detected at 38.9 ppm is assigned to the magnetically inequivalent methyl groups, while quaternary carbon atoms of the *t*Bu groups give rise to a multiplet centred at 40.5 ppm. Similar ^{13}C NMR data were recorded for **1**.† The UV-Vis absorption spectra of **1** and **3** dissolved in THF display two absorption bands in the UV region at 270 nm and 345 nm. The latter absorption tails into the visible region, causing the orange colour of **1** and **3** (see Fig. S39 and S40, ESI†).

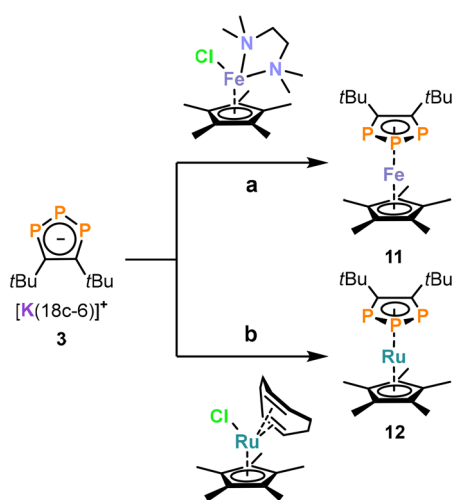## Metal coordination of triphospholide 3: synthesis of iron and ruthenium complexes

Even though several 1,2,3-triphospholide salts were reported, the number of isolated 1,2,3-triphospholyl complexes is

§ Note that the ladderane (*t*BuCP)₄ (*i.e.* the dimer of **A**) does not react with alkali metals under the conditions described in Scheme 1.

limited.[22–25,29,33] To test the utility of the newly synthesized tri-phospholide salts, we investigated the synthesis of triphospha-ferrocenes using **3** (which was selected among **1–5** due to the superior isolated yield).[29,33] Dropwise addition of **3** to [Cp*FeCl(tmeda)] (tmeda = tetramethylethylene-1,2-diamine) afforded the complex [Cp*Fe(η^5-1,2,3-P$_3$C$_2$tBu$_2$)] (**11**, Scheme 2a), which was identified by its AA′X spin system with resonances at 116.3 ppm and at −17.8 ppm in the ^{31}P{^{1}H} NMR spectrum in C$_6$D$_6$. **11** was isolated as a purple powder in 54% yield after work-up. Similarly, the reaction of **3** with [Cp*RuCl(cod)] (cod = cycloocta-1,5-diene) led to the isolation of orange, crystalline [Cp*Ru(η^5-1,2,3-P$_3$C$_2$tBu$_2$)] (**12**) in 32% yield (Scheme 2b). Complex **12** can be identified by two multi-plets (AA′X spin system) at 87.5 ppm and at −39.1 ppm in the ^{31}P{^{1}H} NMR spectrum.

The structural and spectroscopic properties of **11** and **12** are broadly similar to related 1,2,3-triphosphaferrocenes.[29,33b–d] To our knowledge, only one 1,2,3-triphospholide ruthenium complex [K(2,2,2-crypt)][Ru(η^5-P$_3$C$_2$H$_2$){CH$_3$C(CH$_2$)$_2$}$_2$] has been reported so far, which has not been crystallographically characterised.[23] In contrast to the previously reported examples,[29,33b,c] the (phospha-)cyclopentadienyl rings in the structures of **11** and **12** adopt a staggered conformation (Fig. 3), probably due to steric interactions between the Me groups of the Cp* ligands and the tert-butyl groups of the 1,2,3-triphospholyl ligands. It is noteworthy that the planes of the five membered ring ligands are slightly tilted with a plane-to-plane angle of 9°. In both complexes **11** and **12** the bonds in the five-membered ring of the triphospholide ligand are slightly elongated compared to the triphospholide salt **3** (e.g. **3**: P1–P2 = 2.0777(8) Å, C1–C2 = 1.420(3) Å, **11**: P1–P2 = 2.1056(7) Å, C1–C2 = 1.437(3) Å).

Simulation of the ^{31}P{^{1}H} NMR spectra revealed an AA′X spin system for **11** and **12** (Fig. 4). As reported for related complexes,[23,29,33] the ^{31}P and ^{13}C NMR resonances are shifted to lower frequency. The $^1J_{PP}$ coupling constants (**11**: $^1J_{AX}$ =

Fig. 3 Solid-state molecular structures of (a) **11** and (b) **12**. Displacement ellipsoids are drawn at the 50% probability level; H atoms have been omitted for clarity. Selected bond lengths [Å] and angles [°] for **11**: P1–P2 2.1054(7), P2–P3 2.1056(7), P1–C1 1.7999(19), P3–C2 1.8104(19), C1–C2 1.437(3), Fe1–(P$_3$C$_2$)$_{centroid}$ 1.6321(6), Fe1–Cp*$_{centroid}$ 1.7116(9), P1–P2–P3 98.29(3), C1–P1–P2 101.85(6), C2–P3–P2 101.90(6), C1–C2–P3 118.53(13), C2–C1–P1 119.36(14), Cp*$_{centroid}$–Fe1–(P$_3$C$_2$)$_{centroid}$ 172.02(4). **12**: P1–P2 2.1115(8), P2–P3 2.1093(8), P1–C1 1.808(2), P3–C2 1.814(2), C1–C2 1.435(3), Ru1–(P$_3$C$_2$)$_{centroid}$ 1.7595(6), Ru1–Cp*$_{centroid}$ 1.8447(9), P1–P2–P3 98.25(3), C1–P1–P2 101.78(7), C2–P3–P2 101.95(7), C1–C2–P3 118.66(15), C2–C1–P1 119.33(15), Cp*$_{centroid}$–Ru1–(P$_3$C$_2$)$_{centroid}$ 173.19(4).

Fig. 4 (a) Section of the ^{31}P{^{1}H} NMR spectrum of **11** with nuclei assigned to an AA′X spin system; experimental (top); simulation (bottom): δ(P$_X$) = −17.8 ppm, δ(P$_{AA'}$) = 116.3 ppm, $^1J_{AX}$ = −397.1 Hz, $^1J_{A'X}$ = −396.2 Hz, $^2J_{AA}$ = 3.4 Hz. (b) Section of the ^{31}P{^{1}H} NMR spectrum of **12** with nuclei assigned to an AA′X spin system; experimental (top); simulation (bottom): δ(P$_X$) = −39.1 ppm, δ(P$_{AA'}$) = 87.5 ppm, $^1J_{AX}$ = −393.4 Hz, $^1J_{A'X}$ = −393.9 Hz.

Scheme 2 Synthesis of **11** and **12**. Reagents and conditions: (a) THF, −30 °C, 1.5 h; (b) THF, −30 °C, 1.5 h.

397.1 Hz, **12**: $^1J_{AX}$ = 393.4 Hz) are smaller compared to the signals of anionic **3** ($^1J_{AX}$ = 465.6 Hz, vide supra). The UV-Vis absorption spectrum of **11** displays two absorption bands in

the UV region at 240 nm and 280 nm as well as two in the visible region at 470 nm and 575 nm (see Fig. S41 and S42, ESI†).

Oxidation of 3 with Brookhart's acid: synthesis of hexaphosphane 13

Further reactivity studies of **3** with metal salts (*e.g.* [(Ph$_3$P)$_2$NiCl$_2$], [Cp$_3$Ni$_2$]BF$_4$, [(PPh$_3$)CuCl]), oxidizing agents (*e.g.* [Cp$_2$Fe]PF$_6$), and organic electrophiles repeatedly revealed a set of three distinct multiplets at −63.8 ppm, 15.0 ppm and 64.2 ppm (1 : 1 : 1 integral ratio) in the ^{31}P{^{1}H} NMR spectra, which are assigned to a new product **13**. While this pattern was accompanied by further intractable products in most cases, reactions of **3** with [Cp$_2$Fe][BAr$_4^F$] and [H(Et$_2$O)$_2$BAr$_4^F$] (Brookhart's acid, BAr$_4^F$ = B{C$_6$H$_3$(CF$_3$)$_2$}$_4$) gave **13** in a selective fashion (see Fig. S31 and S37, ESI†). Isolation of crystalline **13** was possible from the reaction of **3** with [H(Et$_2$O)$_2$BAr$_4^F$] by extraction of the crude reaction product with *n*-hexane and subsequent recrystallisation from *n*-pentane at −30 °C (22% yield, Scheme 3).

The determination of the molecular structure of **13** by sc-XRD revealed that this complex arises from the dimerisation of two 1,2,3-triphospholyl units, resulting in a tetracyclic structure (Fig. 5). The polycyclic framework of **13** represents a phosphorus-containing isomer of the hydrocarbon hypostrophene (C$_{10}$H$_{10}$) reported by Pettit and co-workers.[34] The P$_6$ core fea-

Scheme 3 Synthesis of **13**.

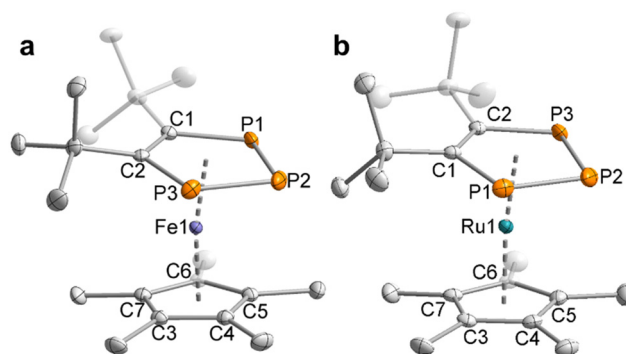**Fig. 5** Solid-state molecular structure of **13**. Displacement ellipsoids are drawn at the 50% probability level; H atoms have been omitted for clarity. Selected bond lengths [Å] and angles [°]: P1–P2 2.1709(8), P1–P6 2.2380(8), P2–P3 2.2082(8), P2–P4 2.2571(8), P3–P5 2.2540(8), P4–P5 2.2054(9), P5–P6 2.1736(9), P1–C1 1.875(2), P3–C2 1.858(2), P4–C3 1.851(2), P6–C4 1.870(2), C1–C2 1.364(3), C3–C4 1.366(3), P1–P2–P3 90.50(3), C1–P1–P2 93.58(7), C2–P3–P2 99.04(7), C1–C2–P3 115.47(15), C2–C1–P1 116.22(15), P4–P5–P6 90.47(3), C3–P4–P5 98.78(7), C4–P6–P5 93.26(7), C3–C4–P6 115.92(15), C4–C3–P4 115.81(16), P1–P2–P4 87.60(3), P3–P2–P4 83.93(3), P4–P5–P3 84.07(3), P6–P5–P3 97.62(3).
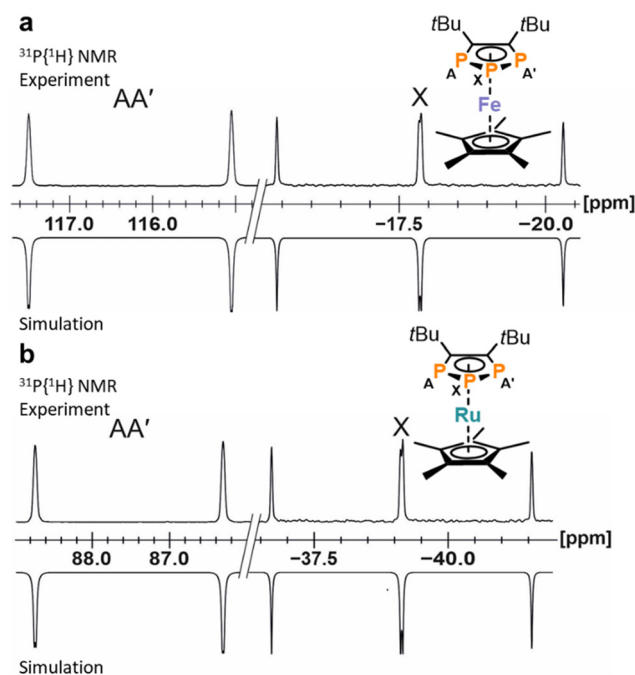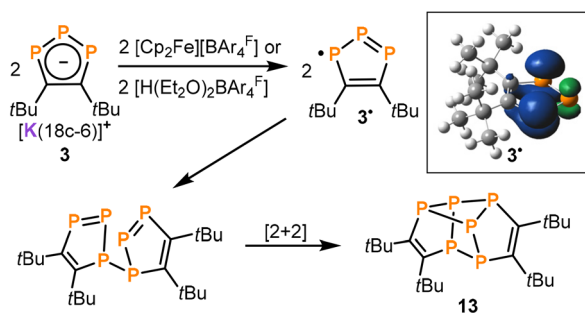
Fig. 6 Sections of the ^{31}P{^{1}H} NMR spectrum of **13** with nuclei assigned to an AA′MM′XX′ spin system; experimental (top); simulation (bottom): δ(P$_{AA'}$) = 64.2 ppm, δ(P$_{MM'}$) = 15.0 ppm, δ(P$_{XX'}$) = −63.8 ppm, $^1J_{AA'}$ = −261.9 Hz, $^1J_{AX}$ = $^1J_{A'X'}$ = −293.9 Hz, $^1J_{M'X}$ = $^1J_{MX'}$ = −134.2 Hz, $^2J_{AM}$ = $^2J_{A'M'}$ = −3.2 Hz, $^2J_{A'M}$ = $^2J_{AM'}$ = 9.9 Hz, $^2J_{MM'}$ = 24.9 Hz, $^2J_{A'X}$ = $^2J_{AX'}$ = 15.3 Hz, $^1J_{MX}$ = $^1J_{M'X'}$ = −157.7 Hz, $^2J_{XX'}$ = 29.5 Hz.

tures a double-envelope arrangement with covalent P–P and P–C single bonds, while the adjacent C atoms each form a C=C double bond (C1–C2 1.364(3) Å, C3–C4 1.366(3) Å).[32] A similar double-envelope P$_6$ moiety has been reported for [Cp″$_2$Th(μ,η^3,η^3-P$_6$)ThCp″$_2$] (Cp″ = η^5-1,3-*t*Bu$_2$C$_5$H$_3$).[35] A related P$_6$ unit is also found in Jutzi's P$_6$(C$_5$Me$_5$)$_2$, which contains an additional P–P bond.[36]

The NMR spectroscopic data of **13** are fully consistent with the molecular structure, revealing two ^{1}H NMR singlets for the chemically inequivalent *t*Bu groups at 1.08 and 1.53 ppm and deshielded ^{13}C nuclei in the five-membered rings (165.0 ppm and 170.5 ppm) consistent with the C=C double bonds. An AA′MM′XX′ spin system is observed in the ^{31}P{^{1}H} NMR spectrum (Fig. 6), confirming the presence of a covalently connected P$_6$ moiety. Note that [Cp″$_2$Th(μ,η^3,η^3-P$_6$)ThCp″$_2$] gives rise to a similar AA′MM′Q$_2$ spin system.[35]

The possible mechanism of formation of **13** is shown in Scheme 4. We presume that [H(Et$_2$O)$_2$BAr$_4^F$] acts as an oxidizing agent towards **3**, forming the radical (1,2,3-P$_3$C$_2$*t*Bu$_2$)$^•$ (**3**$^•$) and dihydrogen (H$_2$) as a by-product.¶ Subsequently, the presumed intermediate **3**$^•$ dimerizes under P–P bond formation, which is followed by a [2 + 2] cycloaddition to generate **13** (Scheme 4). The proposed mechanism is corroborated by DFT calculations (ωB97XD/def2-TZVPPD level of theory) on the

¶We could not unambiguously detect the formation of H$_2$ by ^{1}H NMR spectroscopy. Nevertheless, the well-documented ability of metal phosphides to catalyse hydrogen evolution reactions in acidic media supports the proposed pathway.[37]

Scheme 4 Proposed mechanism for the formation of **13** by oxidation of **3**; the inset shows the calculated spin density distribution of **3˙** drawn at a surface isovalue at 0.05.

radical **3˙**, which show that the calculated spin density is mainly located on the terminal P atoms (P1/P3) of the P_3 chain and to a lesser extent on the central P atom (P2).† An alternative pathway might be the protonation of **3** to form (1,2,3-$P_3C_2tBu_2H$) (**3-H**) that would be prone to cycloaddition, followed by dihydrogen elimination (Scheme S1, ESI†).‖ However, the pathway proposed in Scheme 4 is considered more likely given that **13** from **3** is also formed with aprotic oxidizing agents such as $[Cp_2Fe]PF_6$.†

Conclusions

The reduction of di-*tert*-butyldiphosphatetrahedrane (**A**) offers a new route to 1,2,3-triphospholide salts **1–5**, which are obtained as mixtures with 1,3-diphospholides **6–10**. This contrasts with the direct reduction of *t*BuCP with alkali metals which yields the related 1,2,4-triphospholides in addition to the 1,3-isomers. These findings echo the results of earlier investigations where **A** and *t*BuCP have formed isomeric reaction products.[12] The synthesis of $[Cp*M(\eta^5-1,2,3-P_3C_2tBu_2)]$ (**11**, M = Fe; **12**, M = Ru) from the isolated potassium salt **3** complements earlier studies,[29,33] demonstrating the potential of **3** for transition metal coordination. Furthermore, reactions of **3** with $[Cp_2Fe][BAr_4^F]$ and $[H(Et_2O)_2BAr_4^F]$ resulted in oxidation and dimerisation, forming the hexaphosphane $tBu_4C_4P_6$ (**13**). This compound has a remarkable molecular structure, which is analogous to a hypostrophene ($C_{10}H_{10}$) isomer. These results once more illustrate the potential utility of diphosphatetrahedranes as building blocks in organopho-

sphorus chemistry. Further investigations into the reduction and oxidation of diphosphatetrahedrane **A** are in hand.

Author contributions

MKU: investigation – experimental study and DFT calculations, writing – original draft. GH: conceptualisation, writing – review and editing. GB: investigation – DFT calculations, writing – review and editing. RW: conceptualisation, supervision, funding acquisition, writing – review and editing.

Conflicts of interest

There are no conflicts to declare.

Acknowledgements

References

1. (*a*) K. B. Dillon, F. Mathey and J. F. Nixon, *Phosphorus: The Carbon Copy, From Organophosphorus to Phospha-organic Chemistry*, Wiley, 1998; (*b*) F. Mathey, *Angew. Chem., Int. Ed.*, 2003, **42**, 1578–1604.

2. W. W. Schoeller and T. Busch, *Angew. Chem., Int. Ed. Engl.*, 1993, **32**, 617–619.

3. G. Hierlmeier, P. Coburger, M. Bodensteiner and R. Wolf, *Angew. Chem., Int. Ed.*, 2019, **58**, 16918–16922.

4. M.-L. Y. Riu, R. L. Jones, W. J. Transue, P. Müller and C. C. Cummins, *Sci. Adv.*, 2020, **6**, eaaz3168.

5. M.-L. Y. Riu, M. Ye and C. C. Cummins, *J. Am. Chem. Soc.*, 2021, **143**, 16354–16357.

6. (*a*) G. Maier, S. Pfriem, U. Schäfer and R. Matusch, *Angew. Chem., Int. Ed. Engl.*, 1978, **17**, 520–521; (*b*) G. Maier, *Angew. Chem., Int. Ed. Engl.*, 1988, **27**, 309–332.

7. Selected review articles: (*a*) M. Caporali, L. Gonsalvi, A. Rossin and M. Peruzzini, *Chem. Rev.*, 2010, **110**, 4178–4235; (*b*) B. M. Cossairt, N. A. Piro and C. C. Cummins, *Chem. Rev.*, 2010, **110**, 4164–4177; (*c*) M. Scheer, G. Balázs and A. Seitz, *Chem. Rev.*, 2010, **110**, 4236–4256; (*d*) L. Giusti, V. R. Landaeta, M. Vanni, J. A. Kelly, R. Wolf and M. Caporali, *Coord. Chem. Rev.*, 2021, **441**, 213927; (*e*) C. M. Hoidn, D. J. Scott and R. Wolf, *Chem. – Eur. J.*, 2021, **27**, 1886–1902.

‖ Such a pathway has been proposed by Nixon and co-workers for the protonation of Li[1,2,4-$P_3C_2tBu_2$] with an EtOH/MeCO$_2$H mixture, leading to a tricyclic compound containing a P_5 chain and an isolated P atom.[38] Indeed, our DFT calculations for (1,2,3-$P_3C_2tBu_2$)⁻ show that P1 and P3 have a slightly higher proton affinity than C1, C2 and P2. In contrast, the carbon atoms of (1,2,4-$P_3C_2tBu_2$)⁻ have a higher proton affinity than the phosphorus atoms. The protonation of one P atom in (1,2,3-$P_3C_2tBu_2$)⁻ leads to a localized P=P double bond which is prone to cycloaddition triggering the hydrogen elimination and formation of **13**. Both the dimerisation of **3˙** to **13** and of protonated **3-H** to **13** are exergonic with −59.1 kcal mol⁻¹ and −23.9 kcal mol⁻¹, respectively (see ESI†). A 1,2,4-triphospholide radical dimerisation has been reported by Ionkin and co-workers.[39]

8 G. Hierlmeier, M. K. Uttendorfer and R. Wolf, *Chem. Commun.*, 2021, **57**, 2356–2359.

9 M.-L. Y. Riu, A. K. Eckhardt and C. C. Cummins, *J. Am. Chem. Soc.*, 2022, **144**, 7578–7582.

10 M.-L. Y. Riu, A. K. Eckhardt and C. C. Cummins, *J. Am. Chem. Soc.*, 2021, **143**, 13005–13009.

11 G. Hierlmeier, R. J. Kutta, P. Coburger, H.-G. Stammler, J. Schwabedissen, N. W. Mitzel, M. Dimitrova, R. J. F. Berger, P. Nürnberger and R. Wolf, *Chem. Sci.*, 2024, **15**, 5596–5603.

12 G. Hierlmeier, P. Coburger, D. J. Scott, T. M. Maier, S. Pelties, R. Wolf, D. M. Pividori, K. Meyer, N. P. van Leest and B. de Bruin, *Chem. – Eur. J.*, 2021, **27**, 14936–14946.

13 G. Hierlmeier and R. Wolf, *Angew. Chem., Int. Ed.*, 2021, **60**, 6435–6440.

14 M. K. Uttendorfer, G. Hierlmeier and R. Wolf, *Z. Anorg. Allg. Chem.*, 2022, **648**, e202200124.

15 Reduction chemistry of P₄: (*a*) M. Baudler, D. Düster and D. Ouzounis, *Z. Anorg. Allg. Chem.*, 1987, **544**, 87–94; (*b*) M. Baudler, S. Akpapoglou, D. Ouzounis, F. Wasgestian, B. Meinigke, H. Budzikiewicz and H. Münster, *Angew. Chem., Int. Ed. Engl.*, 1988, **27**, 280–281; (*c*) V. A. Milyukov, A. V. Kataev, O. G. Sinyashin and E. Hey-Hawkins, *Russ. Chem. Bull.*, 2006, **55**, 1297–1299.

16 M. Baudler and J. Hahn, *Z. Naturforsch., B: Chem. Sci.*, 1990, **45**, 1139–1142.

17 Reviews on phosphaalkyne chemistry: (*a*) M. Regitz and O. J. Scherer, *Multiple Bonds and Low Coordination Phosphorus Chemistry*, Thieme, Stuttgart, 1990; (*b*) J. F. Nixon, *Coord. Chem. Rev.*, 1995, **145**, 201; (*c*) K. B. Dillon, F. Mathey and J. F. Nixon, *Phosphorus: The Carbon Copy*, Wiley, Chichester, 1998; (*d*) F. Mathey, *Angew. Chem., Int. Ed.*, 2003, **42**, 1578–1604; (*e*) A. Chirila, R. Wolf, J. C. Slootweg and K. Lammertsma, *Coord. Chem. Rev.*, 2014, **270–271**, 57–74.

18 Examples for the reduction of phosphaalkynes: (*a*) R. Bartsch, P. B. Hitchcock and J. F. Nixon, *J. Chem. Soc., Chem. Commun.*, 1987, 1146–1148; (*b*) R. Bartsch and J. F. Nixon, *Polyhedron*, 1989, **8**, 2407; (*c*) R. Bartsch and J. F. Nixon, *J. Organomet. Chem.*, 1991, **415**, C15–C18; (*d*) S. M. Mansell, M. Green, R. J. Kilby, M. Murray and C. A. Russell, *C. R. Chim.*, 2010, **13**, 1073–1081.

19 The Mg(ɪ) dimer [(nacnac)Mg]₂ (nacnac = HC[C(Me)N(2,6-iPr₂C₆H₃)]₂) reduces phosphaalkynes RCP to 1,3-diphosphacyclobutadienediides [(nacnac)Mg]₂[1,3-P₂C₂R₂]: D. W. N. Wilson, D. D. L. Jones, C. D. Smith, M. Mehta, C. Jones and J. M. Goicoechea, *Dalton Trans.*, 2022, **51**, 898–903.

20 N. Maigrot, M. Sierra, C. Charrier and F. Mathey, *Bull. Soc. Chim. Fr.*, 1994, **131**, 397–399.

21 C. P. Butts, M. Green, T. N. Hooper, R. J. Kilby, J. E. McGrady, D. A. Pantazis and C. A. Russell, *Chem. Commun.*, 2008, 856–858.

22 F. García, R. J. Less, V. Naseri, M. McPartlin, J. M. Rawson, M. Sancho Tomas and D. S. Wright, *Chem. Commun.*, 2008, 859–861.

23 R. S. P. Turbervill and J. M. Goicoechea, *Chem. Commun.*, 2012, **48**, 6100–6102.

24 R. S. P. Turbervill and J. M. Goicoechea, *Inorg. Chem.*, 2013, **52**, 5527–5534.

25 R. S. P. Turbervill, A. R. Jupp, P. S. B. McCullough, D. Ergöçmen and J. M. Goicoechea, *Organometallics*, 2013, **32**, 2234–2244.

26 A. M. Tondreau, Z. Benkő, J. R. Harmer and H. Grützmacher, *Chem. Sci.*, 2014, **5**, 1545–1554.

27 I. A. Bezkishko, A. A. Zagidullin, A. V. Petrov, V. A. Miluykov, T. I. Burganov, S. A. Katsyuba and O. G. Sinyashin, *J. Organomet. Chem.*, 2017, **844**, 1–7.

28 D. Rottschäfer, S. Blomeyer, B. Neumann, H.-G. Stammler and R. S. Ghadwal, *Chem. Sci.*, 2019, **10**, 11078–11085.

29 A. Petrov, L. Conrad, N. T. Coles, M. Weber, D. Andrae, A. Zagidullin, V. Miluykov and C. Müller, *Chem. – Eur. J.*, 2022, **28**, e202203056.

30 I. N. Brago and A. P. Tomilov, *Sov. Electrochem.*, 1968, **4**, 623–625.

31 B. Geissler, S. Barth, U. Bergsträsser, M. Slany, J. Durkin, P. B. Hitchcock, M. Hofmann, P. Binger, J. F. Nixon, P. von Ragué Schleyer and M. Regitz, *Angew. Chem., Int. Ed. Engl.*, 1995, **34**, 484–487.

32 (*a*) F. H. Allen, O. Kennard, D. G. Watson, L. Brammer, A. G. Orpen and R. Taylor, *J. Chem. Soc., Perkin Trans. 2*, 1987, S1–S19; (*b*) D. E. C. Corbridge, *Phosphorus, Chemistry, Biochemistry and Technology*, CRC Press, 2013.

33 (*a*) S. Deng, C. Schwarzmaier, C. Eichhorn, O. Scherer, G. Wolmershäuser, M. Zabel and M. Scheer, *Chem. Commun.*, 2008, 4064–4066; (*b*) O. J. Scherer, T. Hilt and G. Wolmershäuser, *Angew. Chem., Int. Ed.*, 2000, **39**, 1425–1427; (*c*) A. V. Petrov, A. A. Zagidullin, I. A. Bezkishko, M. N. Khrizanforov, K. V. Kholin, T. P. Gerasimova, K. A. Ivshin, R. P. Shekurov, S. A. Katsyuba, O. N. Kataeva, Y. H. Budnikova and V. A. Miluykov, *Dalton Trans.*, 2020, **49**, 17252–17262; (*d*) A. L. Zinnatullin, A. A. Zagidullin, L. I. Savostina, I. A. Bezkishko, A. V. Petrov, E. N. Dulov, R. R. Zairov, V. A. Miluykov and F. G. Vagizov, *Organometallics*, 2023, **42**, 1538–1549.

34 R. Pettit, J. S. McKennis, L. Brener and J. S. Ward, *J. Am. Chem. Soc.*, 1971, **93**, 4957–4958.

35 O. J. Scherer, B. Werner, G. Heckmann and G. Wolmershäuser, *Angew. Chem., Int. Ed. Engl.*, 1991, **30**, 553–555.

36 (*a*) P. Jutzi, R. Kroos, A. Müller and M. Penk, *Angew. Chem., Int. Ed. Engl.*, 1989, **28**, 600–601; (*b*) P. Jutzi, R. Kroos, A. Müller, H. Bogge and M. Penk, *Chem. Ber.*, 1991, **124**, 75–81.

37 R. B. Wexler, J. M. P. Martirez and A. M. Rappe, *ACS Catal.*, 2017, **7**, 7718–7725.

38 R. Bartsch, P. B. Hitchcock and J. F. Nixon, *J. Chem. Soc., Chem. Commun.*, 1989, **15**, 1046–1048.

39 A. S. Ionkin, W. J. Marshall, B. M. Fish, A. A. Marchione, L. A. Howe, F. Davidson and C. N. McEwen, *Eur. J. Inorg. Chem.*, 2008, 2386–2390.